coatings

MDPI

Article

Structural and Mechanical Properties of DLC/TiN Coatings on Carbide for Wood-Cutting Applications

Vadzim Chayeuski [1], Valery Zhylinski [2,*], Victor Kazachenko [3], Aleksandr Tarasevich [2] and Abdelhafed Taleb [4,5]

[1] Department of Physics, Faculty of Information Technology, Belarusian State Technological University, 13a, Sverdlov Str., 220006 Minsk, Belarus
[2] Department of Chemistry, Technology of Electrochemical Production and Electronic Engineering Materials, Chemical Technology and Engineering Faculty, Belarusian State Technological University, 13a, Sverdlov Street, 220006 Minsk, Belarus; altava98@mail.ru
[3] State Enterprise "Science and Technology Park of BNTU "Polytechnic", 37/1, Surganova Str., 220013 Minsk, Belarus; kazachenko@park.bntu.by
[4] Chimie ParisTech, PSL University, CNRS, IRCP, 75005 Paris, France; abdelhafed.taleb@chimieparistech.psl.eu
[5] Sorbonne Université, 4 Place Jussieu, 75231 Paris, France
* Correspondence: zhilinski@yandex.ru; Tel.: +375(17)-378-72-82

Abstract: In this work, the diamond-like carbon and titanium nitride (DLC/TiN) multilayer coatings were prepared on a cemented tungsten carbide substrate (WC—3 wt.% Co) using the cathodic vacuum arc physical vapor deposition (Arc-PVD) method and pulsed Arc-PVD method with a graphite cathode for the deposition of TiN and carbon layers, respectively. The structural and mechanical properties of the prepared coatings were studied, and different techniques, such as scanning electron microscope (SEM), energy-dispersive X-ray spectroscopy (EDX), X-ray diffraction (XRD), Raman spectroscopy, and microindentation techniques investigated their microstructure, composition, and phases. The prepared coatings had a multilayer structure with distinct phases of DLC, TiN, and carbide substrate. The potentiodynamic polarization method (PDP) was performed for the DLC/TiN multilayer coatings in 3% NaCl solution to evaluate the corrosion resistance of the prepared coatings. It has been shown that the DLC layer provided the coating with a polarization resistance of 564.46 kΩ. Moreover, it has been demonstrated that the DLC/TiN coatings had a high hardness of 38.7–40.4 GPa, which can help to extend the wood-cutting tools' life.

Keywords: diamond-like carbon coating; titanium nitride; corrosion resistance; wood-cutting tool

Citation: Chayeuski, V.; Zhylinski, V.; Kazachenko, V.; Tarasevich, A.; Taleb, A. Structural and Mechanical Properties of DLC/TiN Coatings on Carbide for Wood-Cutting Applications. *Coatings* **2023**, *13*, 1192. https://doi.org/10.3390/coatings13071192

Academic Editors: Gianni Barucca and Alexandru Enesca

Received: 26 May 2023
Revised: 30 June 2023
Accepted: 30 June 2023
Published: 2 July 2023

1. Introduction

Nowadays, cemented carbide cutting tools are widely used in wood processing. Although they offer a good ratio of hardness to fracture resistance [1], cemented carbide cutting tools cannot meet the needs of modern wood processing. These tools suffer from problems of high friction, considerable thermal shock, and high-temperature oxidation in the cutting area during the working process [2]. The cutting of wood is very complicated, as the cutting speed is 5 to 20 times higher than that of conventional metal, and the high density of cemented carbide cutting tools can be dangerous when cutting at high speed [3]. In addition, the wood materials are anisotropic and inhomogeneous. Tannins and adhesives in wood products easily corrode cemented carbide-cutting tools [4]. All of this reduces the service life of cutting tools and decreases the efficiency of industrial production.

At this stage, further research is carried out (in addition to the development of new hard alloys and high-speed steels) to protect the surface layer of the tools from wear and maintain its geometry under increased processing conditions [5].

In this context, the research is directed towards the development of new concepts and advanced technologies for the generation of coatings for the cutting tools, which can provide a significant improvement in the operational properties of the cutting tools.

Key directions in this field include the active development of coatings based on nanoscale structure, multilayer composites, gradient coatings, as well as multi-component coatings [6–11]. Studies in the literature reported results on the cutting properties of cemented carbide inserts with monolayer coatings (TiAlVN, TiAlTaN, and TiAlBN), multilayer coatings (TiAlN/TiAlVN, TiAlN/TiAlTaN, and Zr-ZrN-(ZrCrAl)N), as well as nanostructured and gradient Ti-(TiAl)N-(TiAl)N multilayer coatings applied using cathodic vacuum physical vapor deposition (Arc-PVD) technology. The coatings have been developed to guarantee a tool life that is 50% longer on average than that of single-layer coatings for milling steel. The durability of modified milling tools coated by nitride and carbide of Ti, Mo, Zr, Cr, etc., using the Arc-PVD method, is significantly increased at the processing of the wood materials [12,13].

The method based on the simultaneous electrodeposition of metallic coatings and dispersed particles makes it possible to obtain highly effective electrochemical composite coatings (ECC) [14,15]. Currently, carbon-based nanomaterials such as detonation nanodiamonds (DNDs) have unique properties and a wide range of industrial applications. The use of DNDs in the electrochemical deposition of chromium, nickel, zinc, etc., produces coatings with high hardness, wear resistance, and chemical stability [16,17]. It has been reported [18,19] that the promising direction for the use of chromium- and nickel-based ECC with DND is in the reinforcement of wood-cutting tools.

However, depositing diamond coatings on a cemented carbide with a cobalt content (WC-Co) substrate can be complicated due to its poor adhesion. The superior bond strength between substrate and coating in cemented carbide-coated tools is the decisive point in their high durability. Although cobalt as a binder provides additional toughness to the tools made from cemented tungsten carbides, the cobalt contained in cemented carbides can induce graphitization during deposition and consequently have a negative effect on the diamond bonds [20]. Poor adhesion between a diamond coating and a cemented carbide reduces the service life of coated tools. New techniques have been developed to improve the adhesion of diamond-coated carbide tools. The use of multilayers and gradient interfacial transition layers are effective approaches to overcoming the problem of poor adhesion [21]. The TiN coating is often used as a bonding layer to improve the bond strength between the substrate and the outer coating [22,23]. However, TiN coatings undergo significant oxidation at operating temperatures above 500 °C, leading to coating failure [24]. In addition, coatings based on TiN, TiC, etc., and prepared by the Arc-PVD method are known to be porous [20–24]. It has been reported in the literature that diamond coatings suppress the porosity of titanium carbide [25]. Furthermore, it has been shown that the high corrosion resistance of Ti-containing high-entropy alloys can be achieved by the formation of diamond-like films on their surface [26].

Different studies reporting on multilayer coatings synthesized by the combined electroplating and Arc-PVD method have shown that these films have high physical and mechanical properties and that the insertion of DND into the coatings improves their properties [27,28]. The combined treatment of cemented carbide milling cutters (WC—4 wt.% Co) based on electroplating and Arc-PVD methods increased the tool life of ZrC/Ni-DND- and Cr-DND/Mo-N-coated cutting tools by 1.5 to 1.6 times and 1.8 to 2 times, respectively, compared with bare tools when milling laminated chipboard.

Currently, DLC-type coatings are one of the most widely used coatings for reducing wear and friction. In addition, the high chemical resistance of DLC coatings makes them attractive as protective coatings [29–32]. The vapor deposition (PVD) technique is one of the most widely used methods for the industrial processing of DLC coatings, particularly for metal-doped DLC coatings [33–35]. DLC coatings have been used by Grigoriew et al. to improve the strength of ceramic tools [36,37]. It was shown that the strength of Al_2O_3 + TiC-based ceramic plates increased by a factor of 1.4 to 1.6 after the application of DLC PACVD coatings to the turning of 102Cr6 hardened steel. The (CrAlSi)N/DLC-based bilayer coatings synthesized for the experimental samples of SiAlON/TiN and commercial SiAlON ceramic burs reduce the wear rate and increase the durability factor to 1.5 for

ceramic burs compared to uncoated tools when processing the heat-resistant NiCr20TiAl alloy. In addition, these coatings help to improve the quality of the surface layer of the workpiece. Wang N.X. et al. reported that CVD deposition of diamond films on $Mo_{0.5}(TiZrTaW)_{0.5}$ highly concentrated alloy strongly improved corrosion resistance in 3.5 wt.% NaCl and 1 M HCl solutions [38]. This result was explained by the formation of the MC mixed carbide layer [011] (M = Mo, Ti, Ta, and W), which orients the diamond films. This result was explained by the formation of the MC mixed carbide layer [011] (M = Mo, Ti, Ta, and W), which orients the diamond films.

However, DLC coatings on WC-Co-cemented tungsten carbide substrate for wood-cutting applications have not been reported so far. Furthermore, in the real conditions of a particular tool for plate sawing, the main breakage of the knife is the destruction of the cutting tool itself. In addition, the difference in hardening between different manufacturers of coated tools is not very great, in the order of 10 to 15% [29–41].

The aim of the present study is to improve the knives' performance using low-cost hardening coats, since it is necessary to make the technology suitable for mass production. The DLC/TiN coating properties were studied, including phase composition, microstructure, hardness, and corrosion resistance. In addition, the performance of knives with DLC/TiN coatings for cutting wood was assessed.

2. Materials and Methods

The substrates used were commercial knives (Figure 1) manufactured in Germany by the Leitz company. Sample sizes and general view of the sample are shown in Figure 1a,b.

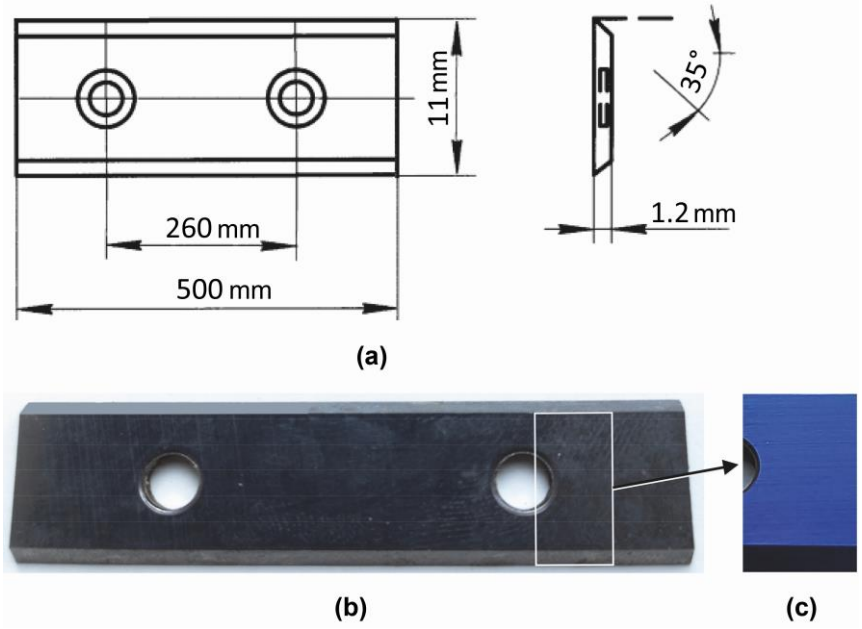

Figure 1. General view with dimensions of the sample (**a**); optical microscopy image of knife with DLC/TiN coating (**b**); DLC/TiN coating (**c**).

The previous studies showed that these knives were made of cemented carbide (WC—3 wt.% Co) [27,28]. The coating deposition process was implemented by the special unit of VP-02 (The State Enterprise "Science and technology park of BNTU "Polytechnic", Minsk, Belarus) [40] using the Arc-PVD method to form the TiN coatings following the standard steps of the method under nitrogen atmosphere [12]. The DLC films were then deposited onto the TiN coatings from the plasma of a pulsed cathodic-arc discharge with a graphite cathode under vacuum [41]. The discharge pulse frequency was 3 Hz and the deposition rate was 15 nm/min. The technological coating process took 45 min. Figure 1c shows a general view of the sample part with the considered DLC/TiN coating.

The structure of the prepared films was characterized by X-ray diffraction (XRD) technique using Ultima IV diffractometer, with Cu-K_α radiation, and at the incidence angle of 1°.

The chemical composition of the coatings and substrate was determined along the cross-section of the coating by the energy-dispersive X-ray spectroscopy (EDS) using Hitachi S-4800 scanning electron microscope (SEM) (Kyoto, Japan). Hitachi S-4800 microscope was also used to identify the microstructure and surface morphology of the deposited coatings.

The diamond-like carbon layer was characterized by Raman spectrometry using Confotec MR-350 confocal laser scanning Raman microscope (Sol Instruments Ltd., Berlin, Germany). The wavelength of the Raman excitation laser was 532 nm, its power was 0.2 mW, and the spectrum recording time was 60 s. The Raman spectra in the wavelength of 1000–1800 cm^{-1} were deconvoluted into D and G Gaussian peaks. The integral area under the D and G peaks was calculated as a function of wavelength and by curve fitting.

The hardness of the coatings was measured using AFFRI-MVDM8 automatic mechanical microhardness tester equipped with the Vickers diamond pyramid indenter. Measurements were performed under the load of 0.5–3.0 N with an accuracy of ±15 HV.

Corrosion studies of the coatings were performed by potentiodynamic polarization (PDP) measurements using AUTOLAB PGSTAT302 N (Utrecht, The Netherlands) in a three-electrode electrochemical cell with a graphite counter electrode and a reference electrode saturated with silver/silver chloride at 25 °C. The surface of the working electrode (1 cm^2) was characterized using a moisture and temperature meter. All potential values measured against the silver/silver-chloride-saturated reference electrode were converted to hydrogen scale. The corrosion resistance of the coatings was estimated using potentiodynamic curves obtained in a 3% NaCl solution (potential sweep rate Vp = 1 mV/s) at an electrode bias of ±800 mV [42,43]. Corrosion currents were calculated using the mathematical modeling functions for the corrosion process in the Nova 2.0 software package (Amsterdam, The Netherlands) and using the polarization resistance method based on the experimental data at the low polarizations (η = ±40 mV):

$$\eta \approx \frac{RT}{nF}\frac{i}{i_0} = R_0 i \quad (1)$$

where $R_0 = \frac{RT}{i_0 nF}$ is the charge transfer resistance, Ohm [43].

The milling method used in the pilot tests was standard milling on a computer numerical control (CNC) processing center RANC-330AE (Klipphausen, Germany) that was equipped with tail mills. The milling head had a cutting diameter of 21 mm and allowed fixing two knives. Knives with 2 cutting edges were removable parts of the mills. The milling of laminated chipboard with a thickness of 16 mm was implemented at cutter rotation frequencies n = 12,000 min^{-1}; feed rate V_F = 4 m/min; and cutting depth h = 1–2 mm. The average billet length was 800 mm, and the appearance of defects in the form of laminate chipped from the plate processing surface was the criterion for losing the cutting ability of the mill knife.

3. Results and Discussion

3.1. Microstructural Analysis

Detailed microstructure studies were performed using EDX analysis. As shown in Figure 2, the DLC/TiN coating exhibits a two-layer structure. The typical fracture morphologies of the samples are shown in Figure 2a, revealing that the coating is composed of two distinct phases corresponding to the carbon-based top layer (Figure 2b) and the TiN layer (Figure 2b–d). The tungsten carbide substrate (WC-Co) is also shown in Figure 2b–d. The TiN coating is not mixed with the carbon-based top film or the substrate. On the top surface, a thin carbon-based layer with a thickness of 198 nm covers the TiN layer and it replicates its relief. Figure 2a shows that the TiN film has a dense and uniform microstructure with columnar growth characteristics and this film exhibits a well-fixed

interface on the carbide substrate. This structure is characteristic of coatings prepared by the Arc-PVD method [44,45]. However, the thickness of the deposited TiN coating is not uniform (Figure 2a), and its thickness is about 2.39–2.75 μm, and the total thickness of the prepared coating varies from 2.59 to 2.95 μm.

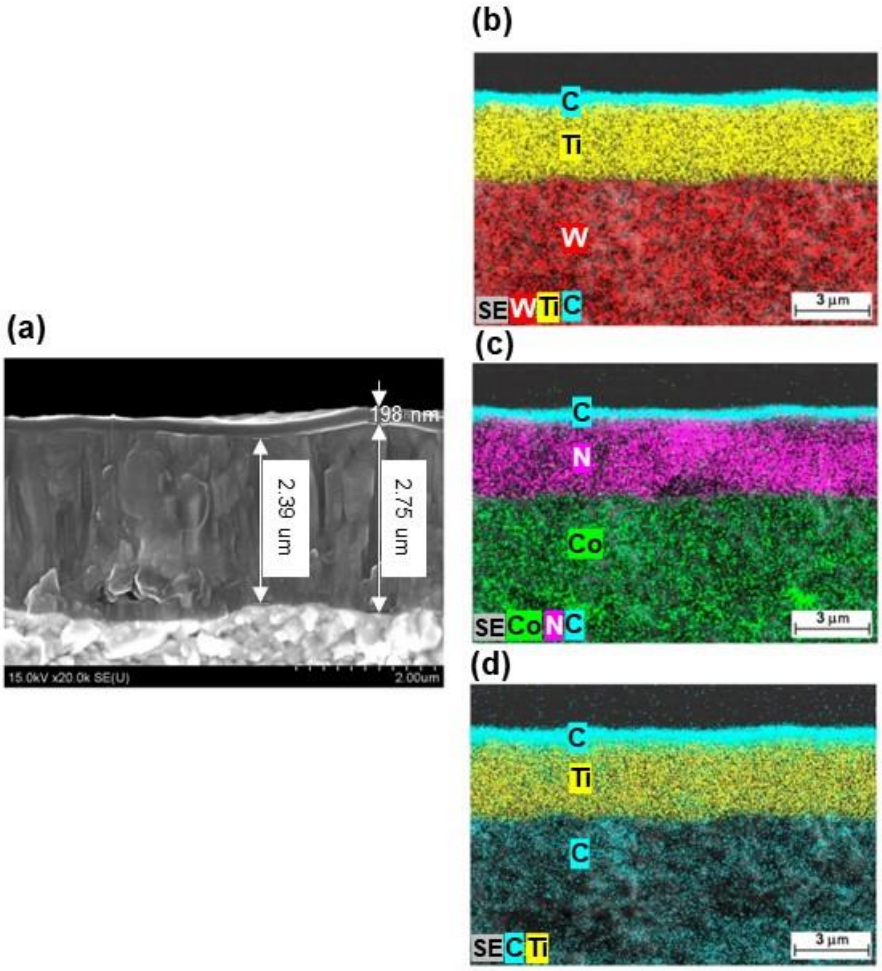

Figure 2. Microstructure of the DLC/TiN coating: (**a**) SEM image and EDS mapping images of the elements (**b**) W, C, and Ti; (**c**) Co, C, and N; (**d**) C and Ti.

3.2. Surface Morphology

Figure 3a shows the surface morphology of the substrate coated by the prepared coating based on the TiN and DLC layers. The surfaces of the TiN and DLC layers are both characterized by a similar structure with the reproduction of a typical knife substrate surface. All films are found to be dense, although a few microparticles are distributed on the surface of the TiN coating (Figure 3a). It is known that these particles may originate from the emission of macroparticles during the deposition of the coating by vacuum cathodic arc using the Arc-PVD method.

Figure 3c shows the high density of the surface structure of the DLC/TiN film without the presence of cracks, cavities, etc. Such relatively uniform surface of relief is evidence that the preparation parameters of the DLC layer of the studied coating were well chosen from previous studies [39,46].

EDS data on the surface composition of the coatings (Figure 3b,d) reveal a high percentage of carbon in the surface layer of the DLC/TiN coating (Figure 3b), whereas the surface composition of the TiN coating contains no carbon (Figure 3d). These experimental results can be understood by the fact that the prepared DLC layer completely covered the TiN layer. The EDS spectrum of the top layer of the DLC/TiN coating shows (Figure 3d) that it contains 32.09 ± 3.9 wt.% carbon (DLC).

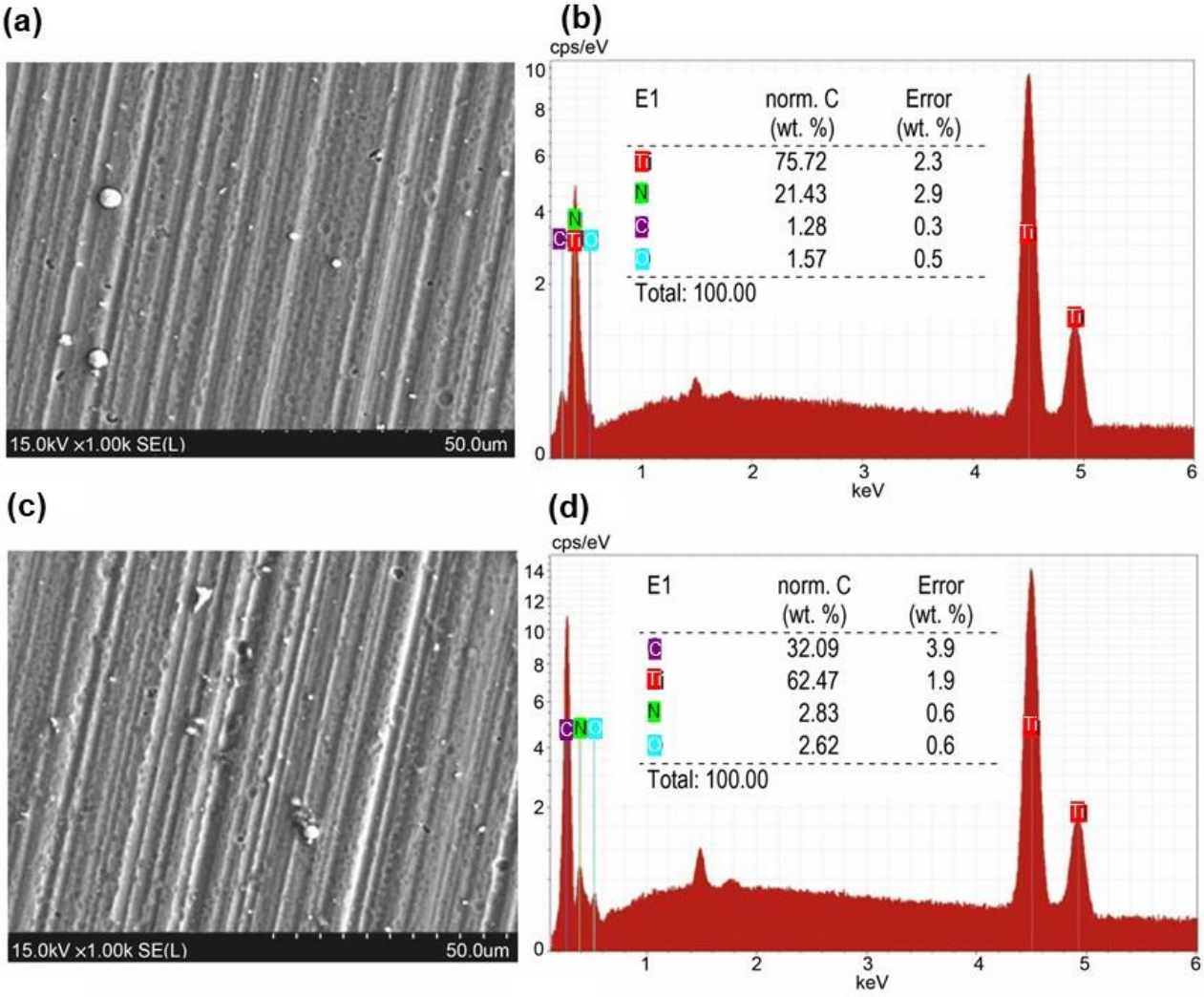

Figure 3. SEM images of coating surfaces (left), EDS spectrum and elemental composition table, corresponding (right): (**a**) TiN coating surface; (**b**) TiN coating surface composition; (**c**) DLC/TiN coating surface; (**d**) DLC/TiN coating surface composition.

3.3. Phase Analysis

Figure 4 shows the XRD spectrum of the DLC/TiN coating. Phase analysis of the coated samples reveals that the most intense diffraction peaks originate mainly from the c-TiN phase. On the other hand, the TiN-coated sample contains an insignificant amount of α-Ti phase, which may belong to traces of Ti microparticles on the coating surface. The WC phase of the substrate (WC-Co alloy) was also detected.

The XRD pattern also showed peaks corresponding to the (111), (220), and (311) crystallographic planes of bonded synthetic diamond [47,48]. It should be noted that the intensity of the peaks is different from that of the natural diamond peaks [49,50], which we explained by the fact that the crystal lattice of synthetic diamonds could be distorted [50]. The positions of the phase reflections also indicate the presence of the graphite phase. The structure of synthesized diamonds is well known in the literature [49,50] and it is characterized by a distorted structure surrounded by disordered (amorphous) graphite shells of carbon atoms linked by sp^3/sp^2 hybrid bonds [51].

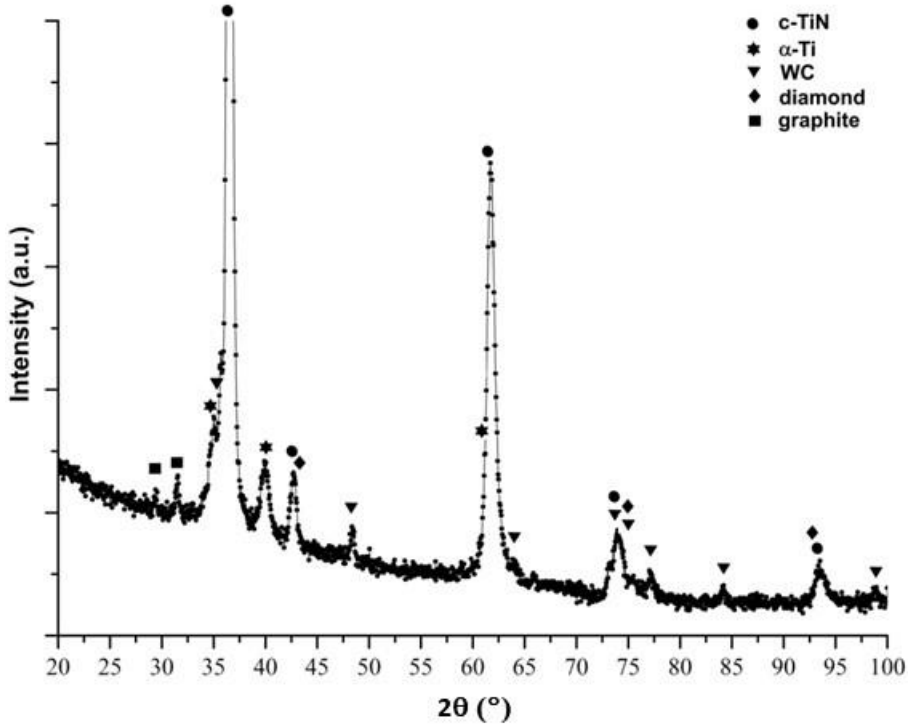

Figure 4. XRD pattern of the DLC/TiN coating sample.

3.4. Raman Spectroscopy

The Raman spectrum of the DLC coating shows a broad asymmetric peak in the range 1100–1800 cm^{-1} (Figure 5), which was well approximated by the two Gaussian fitting results (D and G peaks, Figure 5). It is known that the Raman spectra of DLC films generally match the spectra of graphite when the G peak is above the D peak [29,52–55]. In the present case, the G line was identified as the most prominent line and was associated with the central mode of crystalline graphite clusters. The position of the D peak at 1353 cm^{-1} most likely indicates the presence of crystalline diamond clusters, since the edge modes of disordered graphite give the D line at 1400 cm^{-1} [54], whereas the graphite clusters are small and strongly distorted by the bonds and angles between them [52].

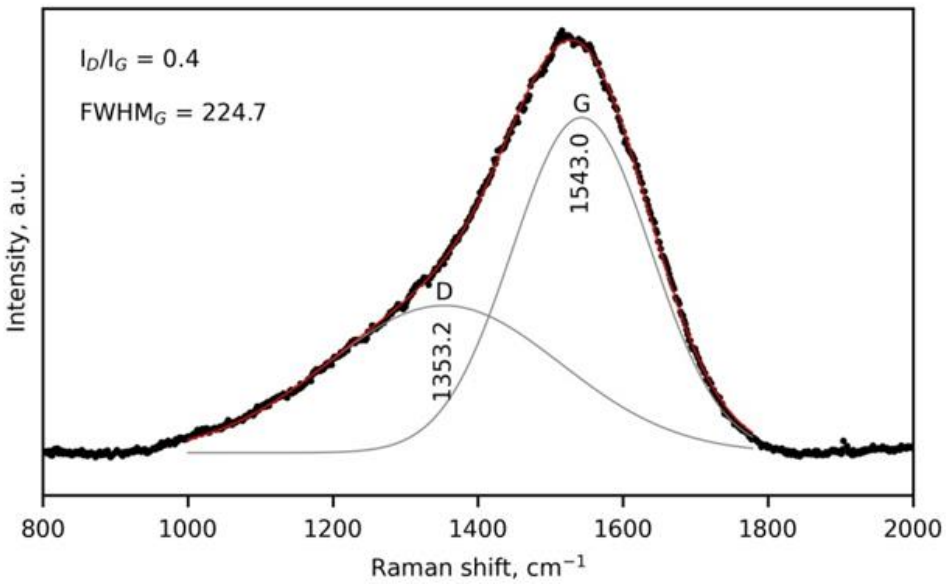

Figure 5. The Raman spectrum of the DLC/TiN coating and the results of its Gaussian fitting.

However, the I_D/I_G intensity ratio was 0.4 (Figure 5), which was associated with a low concentration of sp^3-hybridized carbon atoms of tetrahedral structure and a concentration of sp^2 C–C bonds greater than 70%. [52]. The large number of sp^2-hybridized carbon atoms is due to the presence of graphite-type structures with aromatic group bonds in the carbon layers [29,52].

In our opinion, the significant change detected in the ratio of sp^3 and sp^2 contents in the carbon phase is related to the formation of the graphite-like structures on the titanium nitride surface during the first stage of DLC coating deposition, which is in good agreement with the literature [29,55]. The positions of both the D peak at 1353 cm^{-1} and of the G peak at 1543 cm^{-1} and their half-widths (225 cm^{-1}), as well as the value of their intensity ratio (I_D/I_G) of 0.4, confirm the presence of a diamond-like structure in the deposited carbon layer.

3.5. Corrosion Resistance

Corrosion of the hard coating based on tungsten carbide and titanium nitride is observed at high temperatures ranging from 500 to 700°C in the presence of oxygen [56–58] and under abrasive wear conditions when cutting chipboard panels. Potentiodynamic polarization (PDP) measurements were carried out in a 3% NaCl solution to assess the corrosion resistance of tungsten carbide alloy (WC—3wt.% Co) and TiN and DLC/TiN-based hard coatings. The corrosion test results for the TiN and DLC/TiN coatings on the WC-Co-cemented tungsten carbide surface are shown in Figure 6 and Table 1.

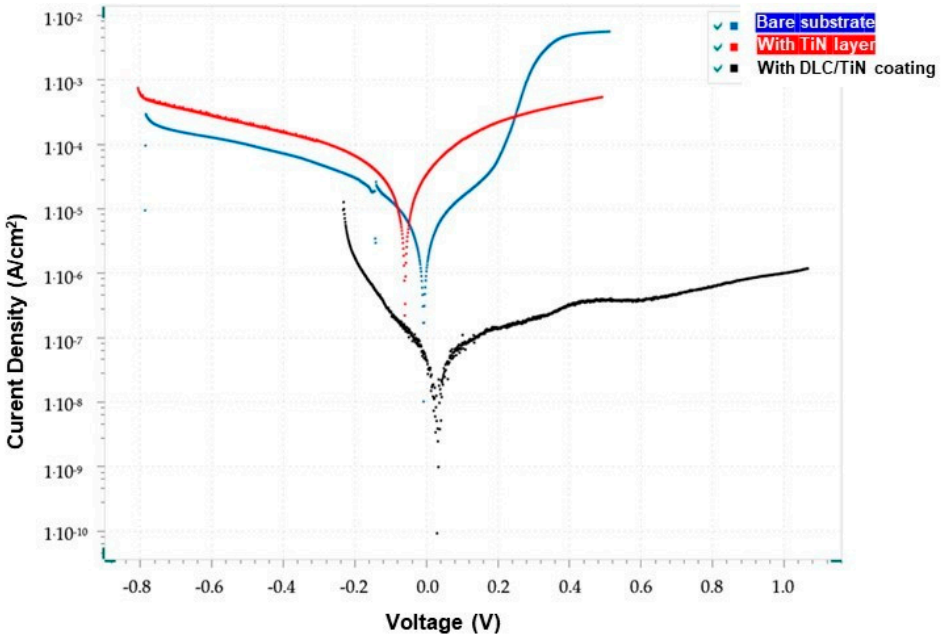

Figure 6. Potentiodynamic curves of the TiN and DLC/TiN coatings on the cemented tungsten carbide (WC—3 wt.% Co) in the 3% aqueous solution of NaCl at v_p = 1 mV/s.

Table 1. Corrosion parameters of the TiN, DLC/TiN coatings on the tungsten carbide alloy (WC-Co) substrate in a 3% aqueous NaCl solution at 25 °C, determined by the polarization resistance method.

Number of Samples	Coating	Corrosion Potential E (V)	Corrosion Current Density i_{corr} (μA/cm²)	Corrosion Penetration D, μm/year	Polarization Resistance R_0 (kOhm)
1	uncoated	−0.006	3.612	21.10	7.20
2	TiN	−0.058	13.375	91.52	1.95
3	TiN/DLC	+0.042	0.046	0.31	564.46

The quasi-equilibrium potential value of the corrosion process of the WC-Co tungsten carbide substrate was −0.006 V and the calculated corrosion current density was 3.612 μA/cm^2 (Table 1), which corresponds to the charge transfer current limit during the corrosion process in the 3% NaCl solution [42]. Oxidation of the tungsten carbide phase was accompanied by the depolarization of the oxygen and the formation of W^{4+} and W^{6+} species, which are soluble in aqueous solutions [56,57]. This resulted in a relatively high corrosion rate of 21.1 μm per year (Table 1). The deposition of the TiN coating on the surface of the tungsten carbide alloy (WC-Co) promoted an increase in corrosion current density to 13.375 μA/cm^2 (Table 1), due to the formation of a titanium dioxide film. This fact showed a pronounced catalytic activity for the oxygen reduction reaction, as reported by other authors in the literature [59–62]. The drastic reduction in corrosion was only observed when the TiN layer was replaced by the DLC/TiN layer (150–200 nm). Under these conditions, the corrosion current density decreased to 0.046 μA/cm^2 and the polarization resistance increased to 564.46 kΩ (Table 1).

These results in terms of improved anticorrosion properties are the consequence of the formation of the dense DLC layer without pores (Figure 2a–d) and with low conductivity. In addition, the increase in the resistance of the DLC layer is due to the formation of C-C sp^3 bonds, which lower the layer conductivity and, in turn, reduce the corrosion process and increase the protective effect of the layer [63–65].

3.6. Mechanical Properties

Characterization of the mechanical properties using the micro indentation technique shows that the microhardness of the TiN layer is between 27.1 and 35.6 GPa, while the microhardness of the DLC/TiN coating is between 38.7 and 40.4 GPa (Table 2). The microhardness values of the TiN layer and the DLC/TiN coating exceed the microhardness of the tungsten carbide alloy substrate (23.5–25.4 GPa) (Table 2). In addition, the microhardness value of the DLC/TiN coating is 1.2–1.4 times and 1.6 times higher than that of the TiN layer and the substrate, respectively. The microhardness values observed for the prepared TiN layer are in good agreement with those reported in the literature for TiN layers prepared by the Arc-PVD technique [66,67].

Table 2. Data of microhardness measurement using the Vickers pyramid indenter.

Number of Samples	Coating	Microhardness at a Load of 200 g (GPa)	Microhardness at a Load of 300 g (GPa)
1	uncoated	25.4	23.5
2	TiN	35.6	27.1
3	DLC/TiN	40.4	38.7

The highest microhardness value of 40.4 GPa was obtained for the DLC/TiN coating. This value is higher than the microhardness of the pure a-C coating (3.66 GPa) deposited on 316L stainless steel by magnetron sputtering technique [29], DLC films prepared by pulsed plasma vapor deposition (8.6 GPa) [39], W-C:H coatings (15.20 GPa) prepared by unbalanced magnetron sputtering in an Ar/C_2H_2 atmosphere on silicon wafers and 440C steel parts [54], and pure DLC (15.9 GPa) fabricated from C_2H_2 gas on silicon wafers using plasma-based ion implantation technique [65].

The increased microhardness of the DLC/TiN coating is due to the high density of the DLC layer (Figure 3c). Studies reported in the literature [34,68] have shown that a high density of the DLC film can significantly improve its mechanical properties. The deposition of DLC/TiN coatings on the surface of cemented carbide substrates (WC—3 wt.% Co) improves the wear resistance of milling tool knife blades, as demonstrated by pilot tests of milling tools with DLC/TiN-coated knives at CJSC Holding "Pinskdrev" (Pinsk, Belarus); six knives were used for each test. This result could be explained by the presence of a diamond-like structure in the deposited carbon layer, as confirmed by the Raman spectroscopy results. Furthermore, it should be noted that the main breakage of the knife is not due

to wear of the reinforcement layers but to fracture of the knives themselves, as has been reported in the literature [34–37,39–41].

Analysis of the durability test results showed differences in the performance of the coatings. The durability of the DLC/TiN-coated tool was 35% higher than that of the bare tool used for cutting laminated chipboard. In addition, the durability of the TiN-coated tool was 18% better than that of the uncoated cutter. The detailed durability procedure was presented in the authors' previous paper [27]. The durability of the cutters was assessed by comparing the values obtained for the total path of contact of the cutter with the machined material for the uncoated and coated cutter [5]. A reported study in the literature [69] showed that the cutter durability (FABA firm) with TiN coatings deposited on WC-4.5 wt.% Co cutters using thermionic arc evaporation was only slightly higher (19%) than that of TiN-coated cutters for chipboard milling in the present work.

4. Conclusions

The DLC/TiN coatings on the edges of the wooden knives were successfully achieved using the Arc-PVD method to prepare the TiN layer and using the pulsed vacuum cathodic discharge plasma method to deposit the DLC layer. The various characterizations showed that the DLC/TiN coatings consist of two distinct layers of DLC (top) and TiN (bottom). The top layer of DLC contains 32.09 ± 3.9 wt.% carbon and has not been mixed with the bottom layer of TiN or the substrate. The thickness of the top DLC layer was measured to be approximately 198 nm, while that of the TiN layer was measured to be around 2.39–2.75 μm, with a total coating thickness of roughly 2.59–2.95 μm. Furthermore, the TiN layer showed a dense and uniform microstructure with columnar growth characteristics and a well-bonded interface to the carbide substrate.

The DLC/TiN coating was characterized by the distinct phases of c-TiN, α-Ti, graphite, and synthetic diamond. The Raman spectrum of the DLC/TiN coating showed the presence of a diamond-like structure in the deposited carbon layer.

The formation of the two-layer DLC/TiN coatings on the cemented tungsten carbide (WC—3wt.% Co) substrate surface significantly improved anticorrosion properties with the reduction in the corrosion current density from 13.375 to 0.046 μA/cm^2 in 3% NaCl. In addition, the two-layer DLC/TiN coating showed an improved microhardness of 38.7–40.4 GPa. Furthermore, application pilot tests on DLC/TiN-coated wood-cutting tools showed that their durability was increased by 35% compared to bare tools when milling laminated chipboard.

DLC/TiN coatings deposited on the surface of cemented carbide (WC—3 wt.% Co) increase the wear resistance of milling tool knife cutters, as demonstrated by pilot tests of milling tools with DLC/TiN-coated cutters at CJSC Holding "Pinskdrev" (Pinsk, Belarus). It was shown that the durability of the cutter is 35% greater than that of a bare cutter when cutting laminated chipboard. It should be noted that the main breakage of the knife is not due to wear of the reinforcement coatings but to fracture of the knives themselves, as has been reported in the literature [30–35,39]. Nevertheless, knives with hardening coatings from different manufacturers showed a 35% increase in performance, encouraging the use of the technology for cost-effective mass production.

Author Contributions: Conceptualization, methodology, V.C.; methodology, V.C. and V.Z.; validation, V.C.; investigation, V.C., V.Z., V.K. and A.T. (Aleksandr Tarasevich); resources, V.C. and V.K.; data curation, V.C., V.Z. and A.T. (Abdelhafed Taleb); writing—original draft preparation, V.C.; writing—review and editing, V.C., V.Z. and A.T. (Abdelhafed Taleb); supervision, A.T. (Abdelhafed Taleb); project administration, V.C.; funding acquisition, V.C. All authors have read and agreed to the published version of the manuscript.

Funding: This research was financed by the State Budget Program of the Republic of Belarus (task no. 8.3 "Technologies of processing and creation of materials by electromagnetism, plasma-beam and foundry-deformation", assignment no. 3.2.7, task no. 8.2. "Nanostructure", assignment no. 2.3).

Institutional Review Board Statement: Not applicable.

Informed Consent Statement: Not applicable.

Data Availability Statement: Data available on request due to privacy or ethical restrictions.

Acknowledgments: The authors would like to express their gratitude to the State Centre "Belmikroanaliz" of the holding company "INTE-GRAL" for providing the necessary facilities for carrying out these studies.

Conflicts of Interest: The authors declare no conflict of interest.

References

1. Guo, X.; Ekevad, M.; Grönlund, A.; Marklund, B.; Cao, P. Tool Wear and Machined Surface Roughness during Wood Flour/Polyethylene Composite Peripheral Up-milling using Cemented Tungsten Carbide Tools. *Bioresources* **2014**, *9*, 3779–3791. [CrossRef]
2. Montenegro, P.; Gomes, J.; Rego, R.; Borille, A. Potential of niobium carbide application as the hard phase in cutting tool substrate. *Int. J. Refract. Met. Hard Mater.* **2018**, *70*, 116–123. [CrossRef]
3. Strehler, C.; Ehrle, B.; Weinreich, A.; Kaiser, B.; Graule, T.; Aneziris, C.G.; Kuebler, J. Lifetime and Wear Behavior of Near Net Shaped Si3N4/SiC Wood Cutting Tools. *Int. J. Appl. Ceram. Technol.* **2012**, *9*, 280–290. [CrossRef]
4. Sommer, F.; Kern, F.; Gadow, R. Injection molding of ceramic cutting tools for wood-based materials. *J. Eur. Ceram. Soc.* **2013**, *33*, 3115–3122. [CrossRef]
5. Zhu, Z.; Guo, X.; Ekevad, M.; Cao, P.; Na, B.; Zhu, N. The effects of cutting parameters and tool geometry on cutting forces and tool wear in milling high-density fiberboard with ceramic cutting tools. *Int. J. Adv. Manuf. Technol.* **2017**, *91*, 4033–4041. [CrossRef]
6. Grigoriev, S.N.; Vereschaka, A.A.; Fyodorov, S.V.; Sitnikov, N.N.; Batako, A.D. Comparative analysis of cutting properties and nature of wear of carbide cutting tools with multi-layered nano-structured and gradient coatings produced by using of various deposition methods. *Int. J. Adv. Manuf. Technol.* **2017**, *90*, 3421–3435. [CrossRef]
7. Volkhonskii, A.O.; Vereshchaka, A.A.; Blinkov, I.V.; Vereshchaka, A.S.; Batako, A.D. Filtered cathodic vacuum Arc deposition of nano-layered composite coatings for machining hard-to-cut materials. *Int. J. Adv. Manuf. Technol.* **2016**, *84*, 1647–1660. [CrossRef]
8. Vereschaka, A.A.; Vereschaka, A.S.; Bublikov, J.I.; Aksenenko, A.Y.; Sitnikov, N.N. Study of Properties of Nanostructured Multilayer Composite Coatings of Ti-TiN-(TiCrAl)N and Zr-ZrN-(ZrNbCrAl)N. *J. Nano Res.* **2016**, *40*, 90–98. [CrossRef]
9. Moganapriya, C.; Rajasekar, R.; Ponappa, K.; Karthick, R.; Perundurai, R.V.; Kumar, P.S.; Pal, S.K. Tribomechanical behavior of TiCN/TiAlN/WC-C multilayer film on cutting tool inserts for machining. *Mater. Test.* **2017**, *59*, 703–707. [CrossRef]
10. Park, I.-W.; Choi, S.R.; Lee, M.-H.; Kim, K.H. Effects of Si addition on the microstructural evolution and hardness of Ti–Al–Si–N films prepared by the hybrid system of arc ion plating and sputtering techniques. *J. Vac. Sci. Technol. A* **2003**, *21*, 895–899. [CrossRef]
11. Kucharska, B.; Sobiecki, J.R.; Czarniak, P.; Szymanowski, K.; Cymerman, K.; Moszczyńska, D.; Panjan, P. Influence of Different Types of Cemented Carbide Blades and Coating Thickness on Structure and Properties of TiN/AlTiN and TiAlN/a-C:N Coatings Deposited by PVD Techniques for Machining of Wood-Based Materials. *Materials* **2021**, *14*, 2740. [CrossRef]
12. Kuleshov, A.K.; Uglov, V.V.; Rusalsky, D.P.; Grishkevich, A.A.; Chayeuski, V.V.; Haranin, V.N. Effect of ZrN and Mo-N coatings and sulfacyanization on wear of wood-cutting knives. *J. Frict. Wear* **2014**, *35*, 201–209. [CrossRef]
13. Chayeuski, V.; Zhylinski, V.; Grishkevich, A.; Rudak, P.; Barcik, S. Influence of High Energy Treatment on Wear of Edges Knives of Wood-Cutting Tool. *MM Sci. J.* **2016**, *2016*, 1519–1523. [CrossRef]
14. Kubrak, P.B.; Drozdovich, V.B.; Zharski, I.M.; Chaevskiy, V.V. Electrodeposition of composite coatings containing car-bon-based nanomaterials and properties of coatings obtained. *Electroplat. Surf. Treat.* **2012**, *XX*, 43–49. (In Russian)
15. Tseluikin, V.N. Tribological properties of composite electrochemical nickel-based coatings. *J. Frict. Wear* **2010**, *31*, 356–358. [CrossRef]
16. Dolmatov, V.Y.; Ozerin, A.N.; Kulakova, I.I.; Bochechka, O.O.; Lapchuk, N.M.; Myllymäki, V.; Vehanen, A. Detonation nanodiamonds: New aspects in the theory and practice of synthesis, properties and applications. *Russ. Chem. Rev.* **2020**, *89*, 1428–1462. [CrossRef]
17. Burkat, G.K.; Dolmatov, V.Y. Application of ultrafine-dispersed diamonds in electroplating. *Phys. Solid State* **2004**, *46*, 703–710. [CrossRef]
18. Polushin, N.I.; Kudinov, A.V.; Zhuravlev, V.V.; Stepareva, N.N.; Maslov, A.L. Dispersed strengthening of a diamond composite electrochemical coating with nanoparticles. *Russ. J. Non-Ferr. Met.* **2013**, *54*, 412–416. [CrossRef]
19. Vityaz, P.A.; Zhornik, V.I.; Ilyushchenko, A.F.; Senyut, V.T.; Komarov, A.I.; Korzhenevskiy, A.P.; Ivakhnik, A.V. *Nanodiamonds of Detonation Synthesis: Preparation and Application*; Belaruskaya Navuka: Minsk, Belarus, 2013. (In Russian)
20. Polini, R.; Barletta, M.; Rubino, G.; Vesco, S. Recent Advances in the Deposition of Diamond Coatings on Co-Cemented Tungsten Carbides. *Adv. Mater. Sci. Eng.* **2012**, *2012*, 151629. [CrossRef]
21. Ma, L.; Yu, X.; Peng, Z.; Fu, Z.; Yue, W.; Wang, C.; Hua, M. Improvement of Film-to-Substrate Adhesion for Diamond and Related Films by Plasma-Based Technologies. *IEEE Trans. Plasma Sci.* **2011**, *39*, 3072–3079. [CrossRef]
22. Wang, M.; Liu, Y.; Chen, H.; Wang, L.; Hu, D. First-Principles Calculations of Interfacial Structure and Properties between WC Substrate and TiN Coating Based on Density Functional Theory. *Coatings* **2022**, *12*, 1076. [CrossRef]

23. Vereschaka, A.; Grigoriev, S.; Tabakov, V.; Migranov, M.; Sitnikov, N.; Milovich, F.; Andreev, N. Influence of the nanostructure of Ti-TiN-(Ti,Al,Cr)N multilayer composite coating on tribological properties and cutting tool life. *Tribol. Int.* **2020**, *150*, 106388. [CrossRef]
24. Chim, Y.C.; Ding, X.Z.; Zeng, X.T.; Zhang, S. Oxidation resistance of TiN, CrN, TiAlN and CrAlN coatings deposited by lateral rotating cathode arc. *Thin Solid Films* **2009**, *517*, 4845–4849. [CrossRef]
25. Gao, J.; Xu, F.; Ma, Z.; Shi, L.; Wang, X.; Zuo, D. Adherent diamond coating deposited on Ti by ultrasonic after carbonization pretreatment. *Proc. Inst. Mech. Eng. Part B J. Eng. Manuf.* **2019**, *10*, 095440541988478. [CrossRef]
26. Han, C.X.; Zhi, J.Q.; Zeng, Z.; Wang, Y.S.; Zhou, B.; Gao, J.; Wu, Y.X.; He, Z.Y.; Wang, X.M.; Yu, S.W. Synthesis and characterization of nano-polycrystal diamonds on refractory high entropy alloys by chemical vapour deposition. *Appl. Surf. Sci.* **2023**, *623*, 157108. [CrossRef]
27. Chayeuski, V.; Zhylinski, V.; Cernashejus, O.; Visniakov, N.; Mikalauskas, G. Structural and Mechanical Properties of the ZrC/Ni-Nanodiamond Coating Synthesized by the PVD and Electroplating Processes for the Cutting Knifes. *J. Mater. Eng. Perform.* **2019**, *28*, 1278–1285. [CrossRef]
28. Chayeuski, V.; Taleb, A.; Zhylinski, V.; Kuleshov, A.; Shtempliuk, R. Preparation and Characterization of the Cr-Nanodiamonds/MoN Coatings with Performant Mechanical Properties. *Coatings* **2022**, *12*, 1012. [CrossRef]
29. Dhandapani, V.S.; Subbiah, R.; Thangavel, E.; Arumugam, M.; Park, K.; Gasem, Z.M.; Veeraragavan, V.; Kim, D.-E. Tribological properties, corrosion resistance and biocompatibility of magnetron sputtered titanium-amorphous carbon coatings. *Appl. Surf. Sci.* **2016**, *371*, 262–274. [CrossRef]
30. Santiago, J.A.; Fernández-Martínez, I.; Sánchez-López, J.C.; Rojas, T.C.; Wennberg, A.; Bellido-González, V.; Molina-Aldareguia, J.M.; Monclús, M.A.; González-Arrabal, R. Tribomechanical properties of hard Cr-doped DLC coatings deposited by low-frequency HiPIMS. *Surf. Coatings Technol.* **2019**, *382*, 124899. [CrossRef]
31. Wang, L.; Liu, Y.; Chen, H.; Wang, M. Modification Methods of Diamond like Carbon Coating and the Performance in Machining Applications: A Review. *Coatings* **2022**, *12*, 224. [CrossRef]
32. Rajak, D.K.; Kumar, A.; Behera, A.; Menezes, P.L. Diamond-Like Carbon (DLC) Coatings: Classification, Properties, and Applications. *Appl. Sci.* **2021**, *11*, 4445. [CrossRef]
33. Evaristo, M.; Fernandes, F.; Cavaleiro, A. Influence of the alloying elements on the tribological performance of DLC coatings in different sliding conditions. *Wear* **2023**, *526-527*, 204880. [CrossRef]
34. Zou, C.W.; Wang, H.J.; Feng, L.; Xue, S.W. Effects of Cr concentrations on the microstructure, hardness, and temperature-dependent tribological properties of Cr-DLC coatings. *Appl. Surf. Sci.* **2013**, *286*, 137–141. [CrossRef]
35. Grigoriev, S.N.; Volosova, M.A.; Vereschaka, A.A.; Sitnikov, N.N.; Milovich, F.; Bublikov, J.I.; Fyodorov, S.V.; Seleznev, A.E. Properties of (Cr,Al,Si)N-(DLC-Si) composite coatings deposited on a cutting ceramic substrate. *Ceram. Int.* **2020**, *46*, 18241–18255. [CrossRef]
36. Grigoriev, S.; Volosova, M.; Fyodorov, S.; Lyakhovetskiy, M.; Seleznev, A. DLC-coating Application to Improve the Durability of Ceramic Tools. *J. Mater. Eng. Perform.* **2019**, *28*, 4415–4426. [CrossRef]
37. Grigoriev, S.N.; Volosova, M.A.; Fedorov, S.V.; Okunkova, A.A.; Pivkin, P.M.; Peretyagin, P.Y.; Ershov, A. Development of DLC-Coated Solid SiAlON/TiN Ceramic End Mills for Nickel Alloy Machining: Problems and Prospects. *Coatings* **2021**, *11*, 532. [CrossRef]
38. Wang, N.X.; Wang, Y.S.; Zheng, K.; Zhi, J.Q.; Zhou, B.; Wu, Y.X.; Xue, Y.P.; Ma, Y.; Cheng, F.; Gao, J.; et al. Achieving CVD diamond films on $Mo_{0.5}(TiZrTaW)_{0.5}$ highly concentrated alloy for ultrastrong corrosion resistance. *Surf. Coatings Technol.* **2023**, *466*, 129620. [CrossRef]
39. Sun, H.; Yang, L.; Wu, H.; Zhao, L. Effects of Element Doping on the Structure and Properties of Diamond-like Carbon Films: A Review. *Lubricants* **2023**, *11*, 186. [CrossRef]
40. Popov, A.N.; Kazachenko, V.P.; Popova, M.A.; Shil'ko, S.V.; Ryabchenko, T.V. Mechanical and Antifrictional Properties of Elastomeric Composites Based on a Rubber for Sealing Elements. *Mech. Compos. Mater.* **2017**, *53*, 505–514. [CrossRef]
41. Kazachenko, V.; Dvorak, A.; Razanau, I.; Li, H. Structure, chemical composition, mechanical properties of fluorine-containing coatings based on diamond-like carbon. *J. Phys. Conf. Ser.* **2018**, *1121*, 012016. [CrossRef]
42. Tao, H.; Zhylinski, V.; Vereschaka, A.; Chayeuski, V.; Yuanming, H.; Milovich, F.; Sotova, C.; Seleznev, A.; Salychits, O. Comparison of the Mechanical Properties and Corrosion Resistance of the Cr-CrN, Ti-TiN, Zr-ZrN, and Mo-MoN Coatings. *Coatings* **2023**, *13*, 750. [CrossRef]
43. Poorqasemi, E.; Abootalebi, O.; Peikari, M.; Haqdar, F. Investigating accuracy of the Tafel extrapolation method in HCl solutions. *Corros. Sci.* **2009**, *51*, 1043–1054. [CrossRef]
44. Sampath Kumar, T.; Balasivanandha Prabu, S.; Manivasagam, G. Metallurgical Characteristics of TiAlN/AlCrN Coating Synthesized by the PVD Process on a Cutting Insert. *J. Mater. Eng. Perform.* **2014**, *23*, 2877–2884. [CrossRef]
45. Vereschaka, A.; Sitnikov, N.; Volosova, M.; Seleznev, A.; Sotova, C.; Bublikov, J. Investigation of Properties of the Zr,Hf-(Zr,Hf)N-(Zr,Hf,Me,Al)N Coatings, Where Me Means Cr, Ti, or Mo. *Coatings* **2021**, *11*, 1471. [CrossRef]
46. Dhandapani, V.S.; Thangavel, E.; Arumugam, M.; Shin, K.S.; Veeraraghavan, V.; Yau, S.Y.; Kim, C.; Kim, D.-E. Effect of Ag content on the microstructure, tribological and corrosion properties of amorphous carbon coatings on 316L SS. *Surf. Coatings Technol.* **2014**, *240*, 128–136. [CrossRef]

47. Dolmatov, V.Y.; Lapchuk, N.M.; Lapchuk, T.M.; Nguyen, B.T.T.; Myllymäki, V.; Vehanen, A.; Yakovlev, R.Y. A study of defects and impurities in doped detonation nanodiamonds by EPR, Raman scattering, and XRD methods. *J. Superhard Mater.* **2016**, *38*, 219–229. [CrossRef]
48. Shen, X.; Wang, X.; Sun, F.; Ding, C. Sandblasting pretreatment for deposition of diamond films on WC-Co hard metal substrates. *Diam. Relat. Mater.* **2017**, *73*, 7–14. [CrossRef]
49. Linnik, S.; Gaydaychuk, A. Processes and parameters of diamond films deposition in AC glow discharge. *Diam. Relat. Mater.* **2013**, *32*, 43–47. [CrossRef]
50. Shishonok, E.M.; Luhin, V.G. XRD Evaluation of Relative Mechanical Strength and Irradiation Resistance of Synthetic Diamond. *J. Mater. Sci. Chem. Eng.* **2015**, *3*, 36–41. [CrossRef]
51. Mykhaylyk, O.O.; Solonin, Y.M.; Batchelder, D.N.; Brydson, R. Transformation of nanodiamond into carbon onions: A comparative study by high-resolution transmission electron microscopy, electron energy-loss spectroscopy, x-ray diffraction, small-angle x-ray scattering, and ultraviolet Raman spectroscopy. *J. Appl. Phys.* **2005**, *97*, 074302. [CrossRef]
52. Robertson, J. Diamond-like amorphous carbon. *Mater. Sci. Eng. R Rep.* **2002**, *37*, 129–281. [CrossRef]
53. Chen, X.; Peng, Z.; Fu, Z.; Wu, S.; Yue, W.; Wang, C. Microstructural, mechanical and tribological properties of tungsten-gradually doped diamond-like carbon films with functionally graded interlayers. *Surf. Coat. Technol.* **2011**, *205*, 3631–3638. [CrossRef]
54. Jun, Z.; Hui, Z.; Zhi-Hua, W.; Rui-Peng, S. Structure and mechanical properties of tungsten-containing hydrogenated diamond like carbon coatings for space applications. *Phys. Procedia* **2011**, *18*, 245–250. [CrossRef]
55. Gershman, I.; Mironov, A.; Mezrin, A.; Torskaya, E.; Kuznetsova, T.; Lapitskaya, V.; Rogachev, A. Effect of sp^3–sp^2 Transformation on the Wear Rate of the DLC Coating. *Lubricants* **2022**, *10*, 85. [CrossRef]
56. Jiang, Y.; Yang, J.; Liu, R.; Wang, X.; Fang, Q. Oxidation and corrosion resistance of WC coated tungsten fabricated by SPS carburization. *J. Nucl. Mater.* **2013**, *450*, 75–80. [CrossRef]
57. Nave, M.I.; Kornev, K.G. Complexity of Products of Tungsten Corrosion: Comparison of the 3D Pourbaix Diagrams with the Experimental Data. *Met. Mater. Trans. A* **2016**, *48*, 1414–1424. [CrossRef]
58. Li, R.; Wang, S.; Zhou, D.; Pu, J.; Yu, M.; Guo, W. A new insight into the NaCl-induced hot corrosion mechanism of TiN coatings at 500 °C. *Corros. Sci.* **2020**, *174*, 108794. [CrossRef]
59. Vega, J.; Scheerer, H.; Andersohn, G.; Oechsner, M. Experimental studies of the effect of Ti interlayers on the corrosion resistance of TiN PVD coatings by using electrochemical methods. *Corros. Sci.* **2018**, *133*, 240–250. [CrossRef]
60. Zhou, D.; Peng, H.; Zhu, L.; Guo, H.; Gong, S. Microstructure, hardness and corrosion behaviour of Ti/TiN multilayer coatings produced by plasma activated EB-PVD. *Surf. Coat. Technol.* **2014**, *258*, 102–107. [CrossRef]
61. Shukla, K.; Rane, R.; Alphonsa, J.; Maity, P.; Mukherjee, S. Structural, mechanical and corrosion resistance properties of Ti/TiN bilayers deposited by magnetron sputtering on AISI 316L. *Surf. Coat. Technol.* **2017**, *324*, 167–174. [CrossRef]
62. Zhang, M.; Niu, Y.; Xin, L.; Su, J.; Li, Y.; Wu, T.; Zhao, H.; Zhang, Y.; Xie, W.; Zhu, S.; et al. Studies on corrosion resistance of thick Ti/TiN multilayer coatings under solid NaCl–H2O–O2 at 450 °C. *Ceram. Int.* **2020**, *46*, 19274–19284. [CrossRef]
63. Freire, F.; Mariotto, G.; Brusa, R.; Zecca, A.; Achete, C. Structural characterization of amorphous hydrogenated carbon and carbon nitride films deposited by plasma-enhanced CVD. *Diam. Relat. Mater.* **1995**, *4*, 499–502. [CrossRef]
64. Sui, J.; Zhang, Z.; Cai, W. Surface characteristics and electrochemical corrosion behavior of fluorinated diamond-like carbon (F-DLC) films on the NiTi alloys. *Nucl. Instrum. Methods Phys. Res. Sect. B Beam Interact. Mater. Atoms* **2009**, *267*, 2475–2479. [CrossRef]
65. Moolsradoo, N.; Watanabe, S. Influence of Elements on the Corrosion Resistance of DLC Films. *Adv. Mater. Sci. Eng.* **2017**, *2017*, 3571454. [CrossRef]
66. Li, B.; Xu, Y.; Rao, G.; Wang, Q.; Zheng, J.; Zhu, R.; Chen, Y. Tribological Properties and Cutting Performance of AlTiN Coatings with Various Geometric Structures. *Coatings* **2023**, *13*, 402. [CrossRef]
67. Tkadletz, M.; Schalk, N.; Daniel, R.; Keckes, J.; Czettl, C.; Mitterer, C. Advanced characterization methods for wear resistant hard coatings: A review on recent progress. *Surf. Coat. Technol.* **2016**, *285*, 31–46. [CrossRef]
68. Khamseh, S.; Alibakhshi, E.; Ramezanzadeh, B.; Sari, M.G. A tailored pulsed substrate bias voltage deposited (a-C: Nb) thin-film coating on GTD-450 stainless steel: Enhancing mechanical and corrosion protection characteristics. *Chem. Eng. J.* **2020**, *404*, 126490. [CrossRef]
69. Kucharska, B.; Czarniak, P.; Kulikowski, K.; Krawczyńska, A.; Rożniatowski, K.; Kubacki, J.; Szymanowski, K.; Panjan, P.; Sobiecki, J.R. Comparison Study of PVD Coatings: TiN/AlTiN, TiN and TiAlSiN Used in Wood Machining. *Materials* **2022**, *15*, 7159. [CrossRef]